



## Photoelectrocatalytic degradation of tetracycline by highly effective TiO<sub>2</sub> nanopore arrays electrode

Yanbiao Liu, Xiaojie Gan, Baoxue Zhou\*, Bitao Xiong, Jinhua Li, Chaoping Dong, Jing Bai, Weimin Cai

School of Environmental Science and Engineering, Shanghai Jiao Tong University, NO. 800 Dongchuan Rd., Shanghai, China

### ARTICLE INFO

#### Article history:

Received 21 April 2009

Received in revised form 8 June 2009

Accepted 11 June 2009

Available online 18 June 2009

#### Keywords:

TiO<sub>2</sub> nanopore arrays

Coated TiO<sub>2</sub> nanofilm

Tetracycline

Photoelectrocatalytic oxidation

### ABSTRACT

The widely utilization of pharmaceutical and personal care products (PPCPs) in the pharmaceutical therapies and agricultural husbandry has led to the worldwide pollution in the environment. In this study, the photoelectrocatalytic (PEC) behaviors of typical PPCPs, tetracycline (TC), were performed via a highly effective TiO<sub>2</sub> nanopore arrays (TNPs) electrode, comparing with electrochemical (EC) and photocatalytic (PC) process. A significant photoelectrochemical synergetic effect in TC degradation was observed on the TNPs electrode and the rate constant for the PEC process of TNPs electrode was ~6.7 times as high as its PC process. The TC removal rate achieved ~80% within 3 h PEC reaction by TNPs electrode, which is ~25% higher than that obtained for a conventional coated TiO<sub>2</sub> nanofilm electrode fabricated by sol–gel method. The possible mechanism involved in the PEC degradation of TC by TNPs electrode was discussed. Furthermore, the TNPs electrode also shows enhanced photocurrent response compared with that for the coated TiO<sub>2</sub> nanofilm electrode. Such kind of TiO<sub>2</sub> nanopores will have many potential applications in various areas as an outstanding photoelectrochemical material.

© 2009 Elsevier B.V. All rights reserved.

## 1. Introduction

TiO<sub>2</sub>-based photocatalytic (PC) and photoelectrocatalytic (PEC) oxidation technique have been proven to be promising and highly efficient processes that can be used to degrade various recalcitrant organic pollutants, such as dyes, pesticides, herbicides, aromatics, etc., under UV light irradiation [1–7]. Upon UV illumination, the electrons are excited from the valence band to the conduction band, generating the electron/hole pairs. The positive holes are powerful oxidants for degrading the organic compounds adsorbed onto the electrode surface. The oxidation efficiency could be further improved by applying a positive bias potential across the electrode, which results in the improved separation of photogenerated electron/hole pairs and better use of photogenerated holes [2,6]. In the past years, the colloidal and particulate titania were widely applied to photodecompose the organic compounds. However, the difficulty in separation and reuse of this catalyst powder from treated water limit its application in practice [8]. To avoid these problems, various pathways [9,10], including sol–gel, sputtering, chemical vapor deposition, etc., have been developed to fabricate TiO<sub>2</sub> nanofilm on the solid supporting substrates. But these TiO<sub>2</sub> materials often suffer from structural disorder and vast grain boundaries, which may bring obstacles to electrons transport and hinder the charge

separation efficiency within the electrode material [2]. In response to these deficiencies, most attempts [11–15] at synthesizing new TiO<sub>2</sub> structures (e.g. TiO<sub>2</sub> nanowires, nanorods, nanobelts, nanorings, nanotubes, etc.) or modifying TiO<sub>2</sub> (e.g. by depositing a noble metal on its surface, sensitizing it with dyes, doping it with transition metals or non-metal elements and complexes with matching semiconductors), have met with certain success.

We have previously reported on the fabrication and characterization of a novel kind of TiO<sub>2</sub> nanopore arrays (TNPs) electrode material with fast separation and transport of photogenerated electron/hole pairs and strong mechanical stability [16,17]. In this paper, we report on an investigation on the PEC degradation of pharmaceutical and personal care products (PPCPs) using the highly effective TNPs electrode and compared with the PEC degradation results obtained using a conventional TiO<sub>2</sub> nanoparticulate film electrode prepared by sol–gel technique and tetracycline (TC) is used as a typical of PPCPs [18,19] (Fig. S1, in Supplementary material). Since TC is widely prescribed in aquaculture and live stocking, can produce a series of pathological changes and disrupt ecosystem equilibrium [18].

## 2. Experimental

### 2.1. Preparation and characterization of the electrode materials

The detailed methodology of preparation highly effective titania nanopores have been published elsewhere [16]. Hence only key

\* Corresponding author. Tel.: +86 21 5474 7351; fax: +86 21 5474 7351.  
E-mail address: [zhoubaoxue@sjtu.edu.cn](mailto:zhoubaoxue@sjtu.edu.cn) (B. Zhou).

points of the fabrication process were summarized here. The titanium sheets (0.25 mm thick, 99.9% purity, Kurumi Works, Japan) were cut into samples of size 20 mm × 50 mm. All anodization experiments were carried out with vigorous magnetic agitation at 5 °C in a two-electrode system (40 mm separation). The anodization voltage was set at 40 V and the electrolyte was dimethyl sulfoxide (DMSO, ≥99.8%) containing 5% HF solution (≥40 wt%). The TNPs can be fabricated by a two-step process: after anodization at 40 V for 70 h, the sample was post-sonicated (KQ-50B, 40 kHz, Kunshan Ultrasonic Instrument Co., Ltd.) for 10 min to remove the uppermost film completely. The obtained TNPs, which are initially amorphous, are crystallized by annealing in an air atmosphere for 8 h at 450 °C with heating and cooling rates of 1 °/min.

Preparation of a colloid of TiO<sub>2</sub> was performed in a basic environment [20,21]. 40.5 mL of titanium tetraisopropoxide was added to 112.5 mL of water at 15 °C with vigorous stirring for 1 h. After washing with distilled water, the product was transferred to a 90 mL solution of 0.02 M tetramethylammonium hydroxide and refluxed at 100 °C for 4 h. The colloid resulting from peptization was treated hydrothermally at 210 °C for 12 h in a Teflon autoclave. After being centrifuged at 5000 rpm and washed with deionized ethanol, the TiO<sub>2</sub> product was dried overnight under an ambient atmosphere at 200 °C. The colloid was then printed onto a SnO<sub>2</sub>/F conductive glass substrate through a screen mesh to form a transparent film. After keeping in an oven at 120 °C for 30 min, the coated TiO<sub>2</sub> film was then calcined in a muffle furnace at 450 °C for 3 h.

The morphologies of the TiO<sub>2</sub> electrodes were studied using a field emission scanning electron microscope (PHILIPS, Netherlands, Sirion 200). The pore depth of the TNPs sample was measured using an atomic force microscope (BioScope) from Veeco Instruments Inc. (USA). The crystallite phase of the electrode materials were investigated with an X-ray diffractometer (Bruker, Germany) using Cu Kα irradiation. A transmission electron microscopy (JEM-2010) was applied to characterize the morphology of the coated TiO<sub>2</sub> nanofilm.

## 2.2. PEC degradation experiments

The PEC experiments were performed in a rectangular shaped quartz reactor (20 mm × 30 mm × 50 mm) using a three-electrode system with a platinum foil counter electrode, a saturated Ag/AgCl reference electrode and a TiO<sub>2</sub> work electrode (Fig. S2, in Supplementary material). The supply bias and work current were controlled using a CHI electrochemical analyzer (CHI 660C, CH Instruments, Inc., USA). A 4 W UV lamp (GE, Japan G4T5) with central wavelength 254 nm was chosen as a UV light source and the illumination area was 20 mm × 20 mm. The PC oxidation reaction was performed by using the same set-up without applying an external potential on the functional electrodes. The PEC degradation of TC experiments were performed under the following conditions: UV irradiation (2.5 mW cm<sup>-2</sup> light intensity), vigorous stirring, 0.5 V

(vs. Ag/AgCl) of electric bias, pH 5.5, 0.02 mol L<sup>-1</sup> sodium sulfate as electrolyte, and no airflow. The initial concentration of TC solution was 10 mg L<sup>-1</sup> and the reaction solution was 20 mL during the experiment. The reaction solution (~3 mL) was quickly withdrawn at given reaction intervals, and was quickly returned to the reactor after being analyzed with a spectrophotometer (UV2102 PCS, UNICO, Shanghai) at 352 nm.

## 3. Results and discussion

### 3.1. Characterization of the electrode materials

Fig. 1a presents the atomic force microscopy (AFM) image of a typical TNPs sample grown from a 5% HF-DMSO electrolyte solution for 70 h at 40 V. It is apparent that the 2D AFM image displays dense and uniform surface morphologies. The line profile in Fig. 1b shows that the average pore depth was ~50 nm. As reported in our previous work [16], the field emission scanning electron microscopy (FE-SEM) image of typical TNPs prepared by Ti anodization in fluorinated DMSO electrolyte at 40 V for 70 h produces a highly ordered nanoporous microstructure, with an average pore diameter of ~220 nm. However, the formation mechanism of TNPs is not yet entirely clear to us. We think it may be ascribed to the following reasons: the long time anodization of titanium in organic electrolytes at low temperature leads to the formation of a layer of nanotubular film, which was completely removed by the following sonication treatment, leaving the special nanoporous microstructure left on the substrate.

In order to compare the PEC capability of the TNPs electrode and the traditional film electrode, a TiO<sub>2</sub> film electrode was fabricated using sol-gel technique [20,21] and Fig. 2a displays the FE-SEM image of a coated TiO<sub>2</sub> nanofilm without heat treatment. It is clearly apparent that the surface of the coated TiO<sub>2</sub> nanofilm exhibited a honeycomb-like structure. The increased roughness of the film is correlated with a high surface area. However, the adherence between the porous TiO<sub>2</sub> nanofilm and the glass substrate is relatively weak, and most nanoparticles are not in direct contact with the support, resulting in the easy recombination of photogenerated electrons and holes during charge separation and transfer process [6]. The transmission electron microscopy (TEM) of the same sample reveals that the titania nanoparticles are homogeneous with grain diameter of ~25 nm (Fig. 2b).

Fig. 3 compares the X-ray diffraction (XRD) patterns of as-annealed TNPs electrode (curve a) and coated TiO<sub>2</sub> nanofilm electrode (curve b). The titanium peaks from substrate and anatase characteristic peaks can be observed for TNPs electrode. The XRD profile of coated TiO<sub>2</sub> nanofilm electrode only contains anatase characteristic peaks. Other titanium phases like the rutile, brookite or amorphous forms, were not found for the two electrode materials.

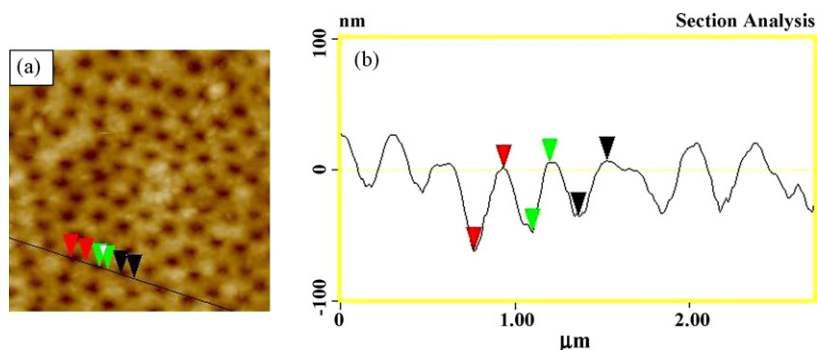


Fig. 1. (a) AFM image of typical TNPs prepared by Ti anodization in 5% HF-DMSO electrolyte solution at 40 V for 70 h; section analysis of the AFM image given in (b).

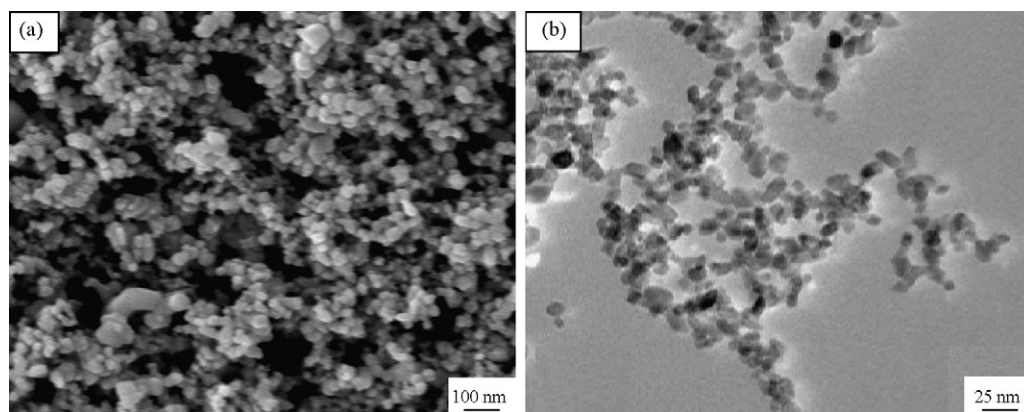


Fig. 2. (a) FE-SEM image of coated TiO<sub>2</sub> nanofilm prepared by sol-gel method; (b) TEM image of the coated TiO<sub>2</sub> nanofilm.

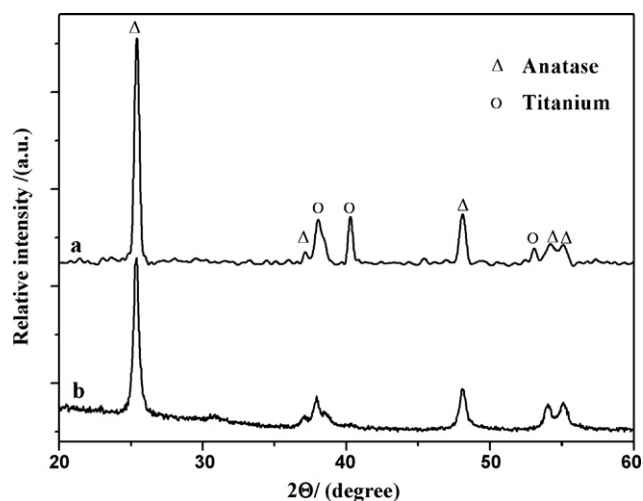


Fig. 3. XRD patterns of as-annealed TNPs electrode (a) and coated TiO<sub>2</sub> nanofilm electrode (b).

### 3.2. Cyclic voltammetry

Fig. 4 shows the results of cyclic voltammograms (CVs) of TNPs electrode (curve a) and coated TiO<sub>2</sub> nanofilm electrode (curve b) in 0.02 M Na<sub>2</sub>SO<sub>4</sub> as a function of applied potential under UV illumination at a scanning rate of 0.02 V s<sup>-1</sup>. By comparing curves

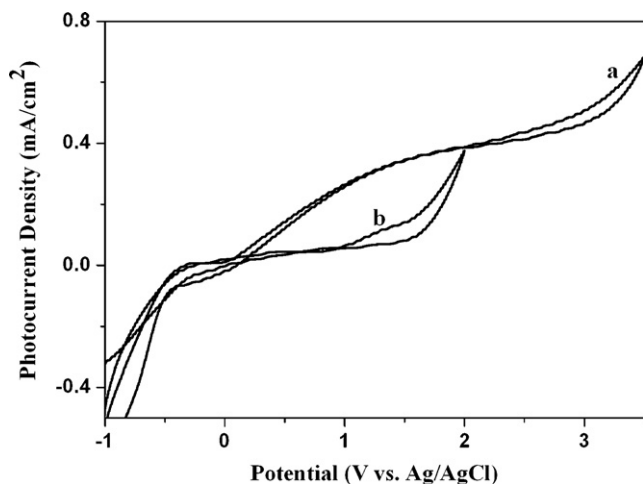


Fig. 4. Cyclic voltammograms (CVs) of TNPs electrode (a) and coated TiO<sub>2</sub> nanofilm electrode (b) in 0.02 M Na<sub>2</sub>SO<sub>4</sub> under UV illumination.

a and b, it is evident that the TNPs electrode (curve a) reveals obviously enhanced photocurrent response and the saturated photocurrent density of TNPs electrode is found ~5.8 times as high as that for coated TiO<sub>2</sub> nanofilm electrode (curve b), indicating that upon the application of an applied potential bias on the TNPs electrode, the separation and transport efficiency of photogenerated electron/hole pairs is much higher than that for coated TiO<sub>2</sub> nanofilm electrode. The dark current for both electrodes is found to be negligible (Fig. S3, in Supplementary material).

### 3.3. PEC degradation of TC by TNPs electrode and coated TiO<sub>2</sub> nanofilm electrode

PEC degradation of TC in aqueous solutions using TNPs electrode and coated TiO<sub>2</sub> nanofilm electrode was present in Fig. 5. In order to quantitatively describe TC degradation in this work, we apply the Langmuir–Hinshelwood (L–H) model, which is usually used to characterize the PC and PEC degradation process of organic compounds [5,22,23]. It is evident that the removal of TC by TNPs electrode and coated TiO<sub>2</sub> nanofilm electrode followed the L–H model satisfactorily (Fig. S4 and Table S1, in Supplementary material). As given in Fig. 5a, within 3 h, ~80% of TC removal ratio was attained for TNPs electrode, while ~55% of TC was removed by the coated TiO<sub>2</sub> nanofilm electrode. The kinetic constants and regression coefficients of TC photoelectrocatalysis by TNPs electrode and coated TiO<sub>2</sub> nanofilm electrode were summarized in Table 1. Table 1 indicates that the kinetic constant of TC oxidation on TNPs electrode ( $0.560 \pm 0.015 \text{ h}^{-1}$ ) was ~50% higher than that on coated TiO<sub>2</sub> nanofilm electrode ( $0.279 \pm 0.006 \text{ h}^{-1}$ ).

A set of typical photocurrent–time (*I*–*t*) profiles obtained during the degradation of TC solution under given conditions were shown in Fig. 6. The photocurrent density observed for TNPs electrode (curve a) is found much higher than that for coated TiO<sub>2</sub> nanofilm electrode (curve b). This result is in accordance with the enhanced CVs response, given in Fig. 4, and improved PEC reactivity, given in Fig. 5, of the TNPs electrode. The photocurrent density directly reflects the photo-efficiency of the photoelectrochemical system and a more effective transport of photogenerated electrons within the electrode material will result in a greater photocurrent response [24]. The enhancement can be ascribed partly to the special nanoporous microstructure of TNPs electrode. Since the properties of functional materials are highly dependent on their microstructure and mechanical stability. Within TNPs, the porous structure is directly connected to the Ti substrate, which avoids the binding between the nanofilm layer and the substrate, as observed in the coated TiO<sub>2</sub> nanofilm electrode. Hence, the TNPs combine with the substrate more directly and with a greater compactness, resulting in a lower transport resistance for photogenerated

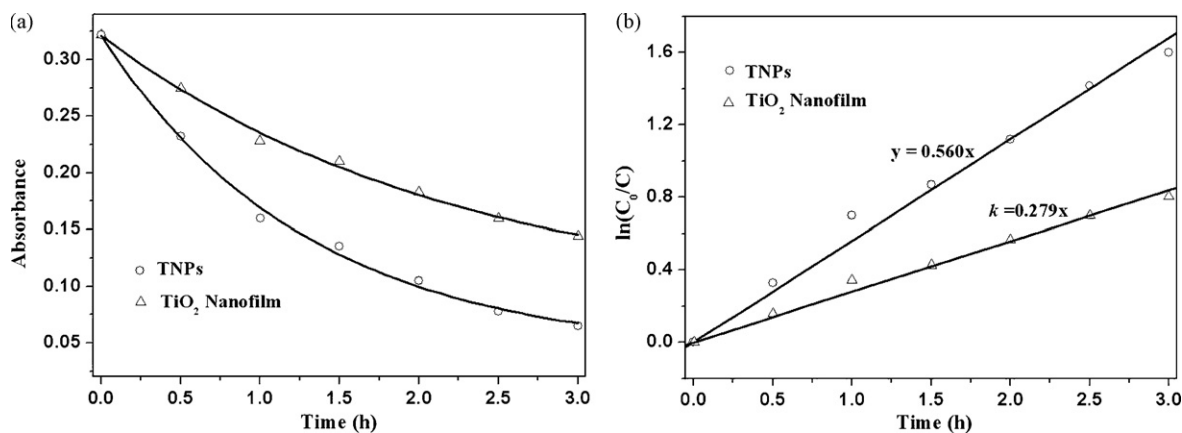


**Fig. 5.** (a) PEC degradation of solutions of TC by TNPs electrode and coated TiO<sub>2</sub> nanofilm electrode; (b) comparison of PEC kinetic curves of TC by TNPs electrode and coated TiO<sub>2</sub> nanofilm electrode.

**Table 1**

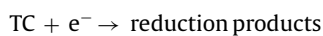
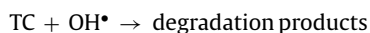
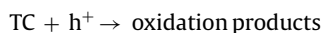
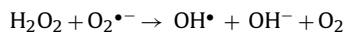
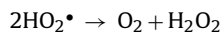
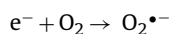
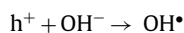
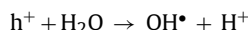
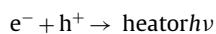
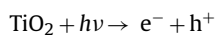
The kinetic constants and regression coefficients of TC photoelectrocatalysis by TNPs electrode and coated TiO<sub>2</sub> nanofilm electrode.

Electrode	Kinetic constant (h <sup>-1</sup> )	R <sup>2</sup>
TNPs	0.560 ± 0.015	0.991
TiO <sub>2</sub> nanofilm	0.279 ± 0.006	0.988

electrons. In addition, such microstructures also show improved mechanical stability, since the TiO<sub>2</sub> is directly attached to the pore walls and there are more supporting points in the nanoporous structure [16]. Therefore, the TNPs electrode is highly effective in its PEC applications compared with the coated TiO<sub>2</sub> nanofilm electrode.

When the TNPs electrode was irradiated with photons of energy equal or greater than its band-gap energy, the conduction band electrons (e<sup>-</sup>) and valence band holes (h<sup>+</sup>) are generated. The photogenerated holes could either recombine with electrons or react with OH<sup>-</sup> or H<sub>2</sub>O oxidizing them into OH• radicals or oxidize the adsorbed TC molecules. The OH• radicals, together with other highly oxidant species are responsible for the decomposition of TC by TNPs electrode. The photogenerated electrons could reduce the adsorbed TC or react with electron acceptors such as O<sub>2</sub> adsorbed on the electrode surface or dissolved in water, reducing it to superoxide radical anion O<sub>2</sub>•<sup>-</sup>, which can be transformed to OH• radicals by further reactions [25–27]. According to this, the possible mechanism involved in the PEC degradation of TC by TNPs electrode can

be expressed as follows:



### 3.4. Comparison of TC degradation by different processes on TNPs electrode

The electrochemical (EC), PC and PEC process of TC in aqueous solutions were performed under given conditions on annealed TNPs electrode. It can be seen in Fig. 7 that, within 3 h, the EC process was obviously much slower than PC and PEC process. The presence of UV light was proven to be effective and ~23% TC was removed within 3 h. When the TNPs electrode was applied an external anodic potential of +0.5 V, TC removal ratio sharply increased to ~80%. Table 2 shows the kinetic constants and regression coefficients of TC degradation by different processes on TNPs electrode. The corresponding reaction rate constant *k* is ranked as: PEC (*k* = 0.560 ± 0.015 h<sup>-1</sup>) > PC

**Table 2**

The kinetic constants and regression coefficients of TC degradation by different processes on TNPs electrode.

Degradation process	Kinetic constant (h <sup>-1</sup> )	R <sup>2</sup>
EC	0.012 ± 0.000	0.999
PC	0.084 ± 0.001	0.995
PEC	0.560 ± 0.015	0.991

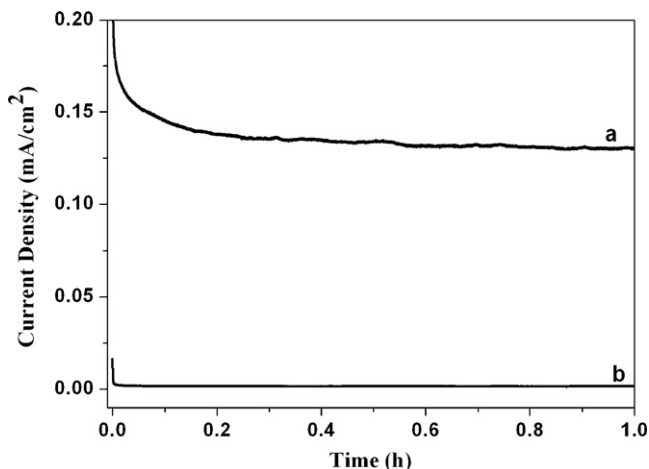


**Fig. 6.** Comparison of photocurrent–time profiles for TC degradation obtained from TNPs electrode (a) and coated TiO<sub>2</sub> nanofilm electrode (b).



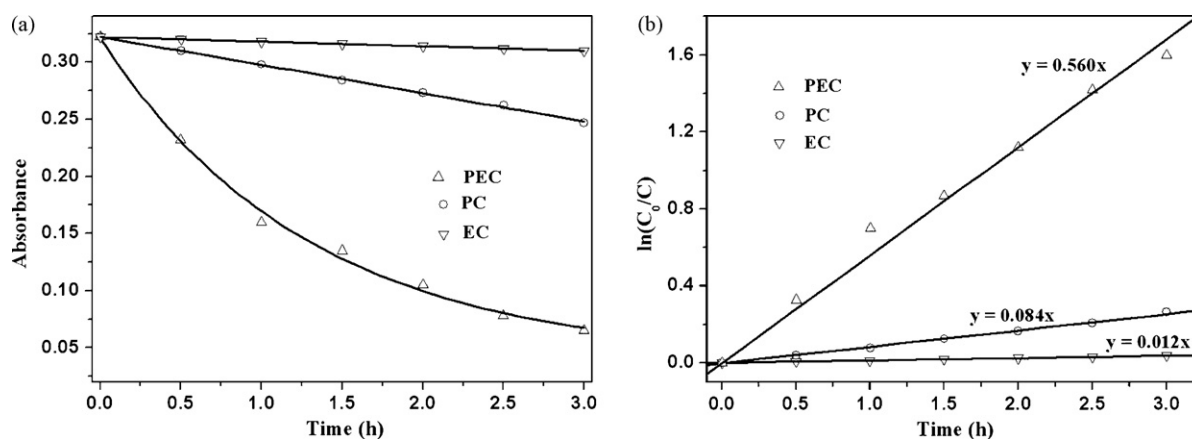


Fig. 7. (a) The EC, PC, and PEC process of solutions of TC on TNPs electrode; (b) comparison of kinetic curves of TC by different processes on TNPs electrode.

( $k = 0.084 \pm 0.001 \text{ h}^{-1}$ ) > EC ( $k = 0.012 \pm 0.000 \text{ h}^{-1}$ ). The obviously enhanced reaction rate constant in the PEC process can be attributed to the suppression of recombination between the photo-generated electron/hole pairs by the external electric field and the special nanoporous microstructure is favorable for the transport of photogenerated electrons. Moreover, there was an evident synergistic effect between the EC and PC process, since the rate constant for the PEC process of TNPs was found  $\sim 6.7$  times as high as that for its PC process.

#### 4. Conclusions

The highly effective titania nanopore arrays were applied as an electrode material in the PEC degradation of TC aqueous solution and the results compared with those obtained using conventional nanoparticulate film electrode. The enhanced photocurrent response and PEC reactivity was obtained for the TNPs electrode. The possible mechanism involved in the PEC degradation of TC by titania nanopores was also discussed. The experimental results suggest that the highly effective TNPs electrode, with strong mechanical stability and superior separation and transport properties of photogenerated electron/hole pairs, may serve well as a promising photoelectrocatalyst and may provide an easy and efficient route to remove PPCPs from wastewater.

#### Acknowledgements

The authors would like to acknowledge the Shanghai Basic Research Key Project (08JC1411300), the National Nature Science Foundation of China (No. 20677039), the State Key Development Program for Basic Research of China (No. 2009CB220004) and the Program of New Century Excellent Talents in University (No. NCET-04-0406) for financial support.

#### Appendix A. Supplementary data

Supplementary data associated with this article can be found, in the online version, at doi:10.1016/j.jhazmat.2009.06.054.

#### References

- [1] Z.Q. Gao, S.G. Yang, N. Ta, C. Sun, Microwave assisted rapid and complete degradation of atrazine using  $\text{TiO}_2$  nanotube photocatalyst suspensions, *J. Hazard. Mater.* 145 (2007) 424–430.
- [2] Z.Y. Liu, X.T. Zhang, S. Nishimoto, M. Jin, D.A. Tryk, T. Murakami, A. Fujishima, Highly ordered  $\text{TiO}_2$  nanotube arrays with controllable length for photoelectrocatalytic degradation of phenol, *J. Phys. Chem. C* 112 (2008) 253–259.
- [3] X. Wang, H.M. Zhao, X. Quan, Y.Z. Zhao, S. Chen, Visible light photoelectrocatalysis with salicylic acid-modified  $\text{TiO}_2$  nanotube array electrode for p-nitrophenol degradation, *J. Hazard. Mater.* 166 (2009) 547–552.
- [4] H.C. Liang, X.Z. Li, Effects of structure of anodic  $\text{TiO}_2$  nanotube arrays on photocatalytic activity for the degradation of 2,3-dichlorophenol in aqueous solution, *J. Hazard. Mater.* 162 (2009) 1415–1422.
- [5] Y.B. Liu, J.H. Li, B. X. Zhou, J. Bai, Q. Zheng, J.L. Zhang, W.M. Cai, Comparison of photoelectrochemical properties of  $\text{TiO}_2$ -nanotube-array photoanode prepared by anodization in different electrolyte, *Environ. Chem. Lett.*, (2008). doi:10.1007/s10311-008-0180-z.
- [6] Q. Zheng, B.X. Zhou, J. Bai, L.H. Li, Z.J. Jin, J.L. Zhang, J.H. Li, Y.B. Liu, W.M. Cai, X.Y. Zhu, Self-organized  $\text{TiO}_2$  nanotube array sensor for the determination of chemical oxygen demand, *Adv. Mater.* 20 (2008) 1044–1049.
- [7] S. Qiao, D.D. Sun, J.H. Tay, C. Easton, Photocatalytic oxidation technology for humic acid removal using a nano-structured  $\text{TiO}_2/\text{Fe}_2\text{O}_3$  catalyst, *Water Sci. Technol.* 47 (2003) 211–217.
- [8] H.F. Zhuang, C.J. Lin, Y.K. Lai, L. Sun, J. Li, Some critical structure factors of titanium oxide nanotube array in its photocatalytic activity, *Environ. Sci. Technol.* 41 (2007) 4735–4740.
- [9] G.L. Puma, A. Bonob, D. Krishnaiahb, J.G. Collin, Preparation of titanium dioxide photocatalyst loaded onto activated carbon support using chemical vapor deposition: a review paper, *J. Hazard. Mater.* 157 (2008) 209–219.
- [10] F.F. Gao, Y. Wang, D. Shi, J. Zhang, M.K. Wang, X.Y. Jing, R. Humphry-Baker, P. Wang, S.M. Zakeeruddin, M. Gratzel, Enhance the optical absorptivity of nanocrystalline  $\text{TiO}_2$  film with high molar extinction coefficient ruthenium sensitizers for high performance dye-sensitized solar cells, *J. Am. Chem. Soc.* 130 (2008) 10720–10728.
- [11] S. Sakthivel, H. Kisch, Daylight photocatalysis by carbon-modified titanium dioxide, *Angew. Chem. Int. Ed.* 42 (2003) 4908–4911.
- [12] D.W. Gong, C.A. Grimes, O.K. Varghese, W.C. Hu, R.S. Singh, Z. Chen, E.C. Dickey, Titanium oxide nanotube arrays prepared by anodic oxidation, *J. Mater. Res.* 16 (2001) 3331–3334.
- [13] B. O'Regan, M. Gratzel, A low cost, high-efficiency solar cell based on dye-sensitized colloidal  $\text{TiO}_2$  films, *Nature* 353 (1991) 737–739.
- [14] Y. Wang, G. Du, H. Liu, D. Liu, S. Qin, N. Wang, C. Hu, X. Tao, J. Jiao, J. Wang, Z.L. Wang, Nanostructured sheets of Ti–O nanobelts for gas sensing and antibacterial applications, *Adv. Funct. Mater.* 18 (2008) 1131–1137.
- [15] G.K. Mor, O.K. Varghese, M. Paulose, K. Shankar, C.A. Grimes, A review on highly ordered, vertically oriented  $\text{TiO}_2$  nanotube arrays: fabrication, material properties, and solar energy applications, *Sol. Energy Mater. Sol. Cells* 90 (2006) 2011–2075.
- [16] Y.B. Liu, B.X. Zhou, J. Bai, J.H. Li, J.L. Zhang, Q. Zheng, X.Y. Zhu, W.M. Cai, Efficient photochemical water splitting and organic pollutant degradation by highly ordered  $\text{TiO}_2$  nanopore arrays, *Appl. Catal. B: Environ.* 89 (2009) 142–148.
- [17] B.X. Zhou, Y.B. Liu, J. Bai, J.H. Li, PR Chinese Patent 200810033302.3 (2008).
- [18] S.J. Jiao, S.R. Zheng, D.Q. Yin, L.H. Wang, L.Y. Chen, Aqueous photolysis of tetracycline and toxicity of photolytic products to luminescent bacteria, *Chemosphere* 73 (2008) 377–382.
- [19] B.J. Richardson, P.K.S. Lam, M. Martin, Emerging chemicals of concern: pharmaceuticals and personal care products (PPCPs) in Asia, with particular reference to southern China, *Mar. Poll. Bull.* 50 (2005) 913–920.
- [20] S.D. Burnside, V. Shklover, C. Barbe, P. Comte, F. Arendse, K. Brooks, M. Gratzel, Self-organization of  $\text{TiO}_2$  nanoparticles in thin films, *Chem. Mater.* 10 (1998) 2419–2425.
- [21] B.T. Xiong, B.X. Zhou, L.H. Li, J. Cai, Y.B. Liu, W.M. Cai, Preparation of nanocrystalline anatase  $\text{TiO}_2$  using basic sol–gel method, *Chem. Papers* 62 (2008) 382–387.
- [22] Z.H. Zhang, Y. Yuan, G.Y. Shi, Y.J. Fang, L.H. Liang, H.C. Ding, L.T. Jin, Photoelectrocatalytic activity of highly ordered  $\text{TiO}_2$  nanotube arrays electrode for azo dye degradation, *Environ. Sci. Technol.* 41 (2007) 6259–6263.

- [23] X. Quan, S.G. Yang, X.L. Ruan, H.M. Zhao, Preparation of titania nanotubes and their environmental applications as electrode, *Environ. Sci. Technol.* 39 (2005) 3770–3775.
- [24] D.L. Jiang, H.J. Zhao, S.Q. Zhang, R. John, Characterization of photoelectrocatalytic processes at nanoporous TiO<sub>2</sub> film electrodes: photocatalytic oxidation of glucose, *J. Phys. Chem. B* 107 (2003) 12774–12780.
- [25] D.D. Sun, J.H. Tay, K.M. Tan, Photocatalytic degradation of *E. coliform* in water, *Water Res.* 37 (2003) 3452–3462.
- [26] V. Iliev, D. Tomova, L. Bilyarska, A. Eliyas, L. Petrov, Photocatalytic properties of TiO<sub>2</sub> modified with platinum and silver nanoparticles in the degradation of oxalic acid in aqueous solution, *Appl. Catal. B: Environ.* 63 (2006) 266–271.
- [27] I.K. Konstantinou, T.A. Albanis, TiO<sub>2</sub>-assisted photocatalytic degradation of azo dyes in aqueous solution: kinetic and mechanistic investigations, *Appl. Catal. B: Environ.* 49 (2004) 1–14.